Journal of Directed Energy, **3**, Spring 2009, 107–117

Two-Dimensional Re-Imaging Assisted Phased Array Architecture for Coherent Beam Combination

Andrew Bratcher and Radoslaw Uberna*

Lockheed Martin Coherent Technologies, 135 S. Taylor Avenue, Louisville, Colorado 80027

Many applications, most notably directed energy applications, call for high-power lasers with good beam quality. Current roadblocks of solid-state and fiber laser technology limit the amount of power that can be achieved in a single diffraction-limited output. One technique to increase the total output power of a laser system is to combine multiple lower power lasers into a single, high-power beam. A Re-imaging Assisted Phased Array Architecture (REAPAR) based on self-imaging waveguides was recently developed at Lockheed Martin Coherent Technologies (LMCT) and implemented to coherently combine multiple laser beams in waveguides. Beam combination in a waveguide has the ability to produce a single diffraction-limited spot without the sidelobes typical of a free-space phased array, theoretically enabling lossless combination. Prior work at LMCT investigated the suitability and combining efficiency of one-dimensional waveguides, and recent thrusts of the REAPAR concept have extended to beam combination in two-dimensional (2-D) waveguides. We present the recent results of the combination of four fiber-launched beams in a 2-D hollow glass waveguide with the opportunities for improved efficiency.

KEYWORDS: Beam combination, Phased array, Self-imaging, Waveguide

1. Introduction

A key research interest in the directed energy community has focused on the development of high-energy lasers (HELs). The push for ever-higher power levels out of a laser system, while still maintaining good beam quality, has recently resulted in kilowatt-level systems. Lower limits of power for small-scale missions, however, target a 100-kW-class laser with good beam quality.[14,19] One approach to achieving such high power levels aims to combine the outputs of multiple laser systems into a single beam.[1–4,7–20] A coherent combination of many laser beams into a single, diffraction-limited output has the potential to achieve high power levels as well as maintain the beam quality necessary for directed energy applications.[1,3,4,7–10,12,14,15,18,20] The most straightforward architecture for coherent combination is a free-space phased array, in which a two-dimensional (2-D) array of sources, with proper phasing between the sources, will interfere constructively in the far field into a

Received September 4, 2008; revision received January 29, 2009.
*Corresponding author; e-mail: radek.uberna@lmco.com.

dominant central lobe. However, appreciable sidelobes will sink a considerable portion of the output power.[4,7–10,14]

Fiber lasers present an attractive choice for combination. Fiber lasers can be designed to be highly efficient (both optically and thermally), as well as produce near-diffraction-limited outputs, given the correct choice of launch fiber. Their small size enables close packaging of individual fiber elements into array formats. For these reasons, fiber lasers are often utilized in phased array combination schemes.

Lockheed Martin Coherent Technologies' (LMCT) Re-imaging Assisted Phased Array (REAPAR) architecture, based on Talbot self-imaging in a waveguide, addresses the shortcomings of free-space phased arrays.[4,8–10] The REAPAR architecture combines an array of sources through a waveguide, relying on the multimodal interference that takes place down the guide. With proper phase control of the input sources, the beams constructively interfere into a diffraction-limited output beam free of power-sinking sidelobes. With the absence of sidelobes, all of the input power is combined into the single central output beam, theoretically enabling lossless beam combination.

Prior work at LMCT has focused on beam combination in one-dimensional (1-D) metallic waveguides. Large, curved, tapered transport waveguides were used to deliver free-space optical beams into a combining waveguide. 1-D combination of two and four beams was demonstrated producing an output Strehl ratio of >0.7 and up to 83% combining efficiency.[8] The scalability in the number of beams in the 1-D configuration is limited by size constraints, as the combining waveguide length can become quite long with the addition of beams. To reduce the size and weight of the four-to-one combiner, as well as enable scaling to higher beam count more practical, 2-D architecture was developed.[4,9] To eliminate the large transport waveguides and fit the geometry of 2-D combination, fiber arrays were developed to serve as input sources. The added benefit of a fiber launch array is the ability to directly couple, via standard connection or splice, the outputs of high-power fiber amplifier systems to a beam-combining waveguide. Here, we present a brief description of Talbot imaging in a waveguide, recent results of four-beam combination, and a path to further optimize the combining efficiency of our system.

2. Theory and Simulation

Self-imaging of a periodic array of objects is a well-known phenomenon that was first observed in the early 1800s by Talbot.[21] Bryngdahl first suggested that images could form in a waveguide,[5,6] with Ulrich and Ankele exploring the phenomenon in more detail and showing the first experimental observation of self-imaging in a waveguide.[22] Briefly, in free space, the illumination of an array of objects by a coherent plane wave will cause a self-image of the objects at integer multiples of the Talbot length due to the diffraction of the wave around the images. The Talbot length is that distance at which constructive interference of the diffracted wavefronts from the objects occurs. Inside a waveguide, a single input source will excite many higher order modes inside the guide. These higher order modes appear to come from an array of virtual sources in the same plane as the original input, mimicking the free-space array configuration. The higher order modes will interfere down the length of the guide constructively at integer multiples of the Talbot length. For a 2-D square waveguide of cross-section a, the self-imaging length is

$$T_L = \frac{4na^2}{\lambda},$$

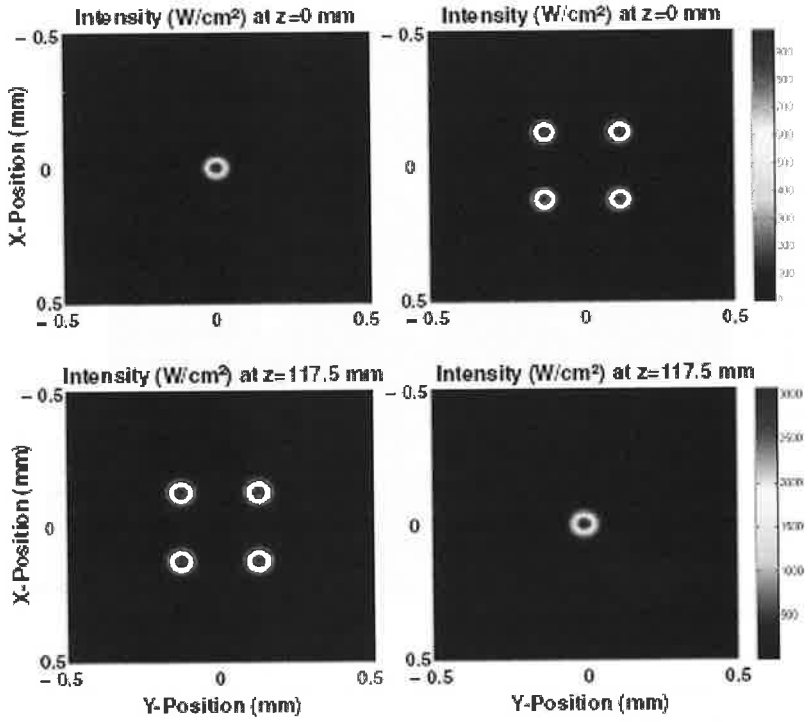

Fig. 1. Model of the waveguide used as a beam splitter (left-hand panels) and beam combiner (right-hand panels). The top pictures show the input beam(s), and the bottom pictures show the output profiles of the waveguide.

with λ being the wavelength of the light and n the refractive index of the guiding structure ($n = 1$ for a hollow waveguide). Of note for beam combination was Ulrich and Ankele's experimental observation of predicted subimage (or Fresnel image) formation at fractional Talbot distances in waveguides.[22] At these fractional Talbot distances, an input beam, centered on the input aperture, will break up into multiple axially symmetric beams. By inputting an array of sources at the correct subimage positions in a waveguide with proper cross-sectional geometry and length, along with the correct phasing between the sources, the self-imaging process can be employed to combine the array of input beams into a single output beam.

The re-imaging conditions in a waveguide were theoretically verified by modeling the beam propagation in the guiding structure. Figure 1 shows some of the results of the simulations. First, the waveguide was modeled as a beam splitter, with one beam input. The model predicts the input beam splitting into four output beams at one-eighth of the Talbot length. The phase profile map of the output in Fig. 2 shows that the four beams have a uniform phase. Next, the process was run in reverse, with four cophased beams input. The output, as expected, depicts a combination of the four beams into a single output beam (Fig. 1, right-hand panels). An interesting result occurs when the phase profiles of the four input beams are adjusted. By offsetting the phase of two diagonal beams by a half-wave at the input, the resulting output pattern shows that the input beam 2×2 array simply re-images down the length of the guide at the output, as shown in Fig. 3. With all the beams being

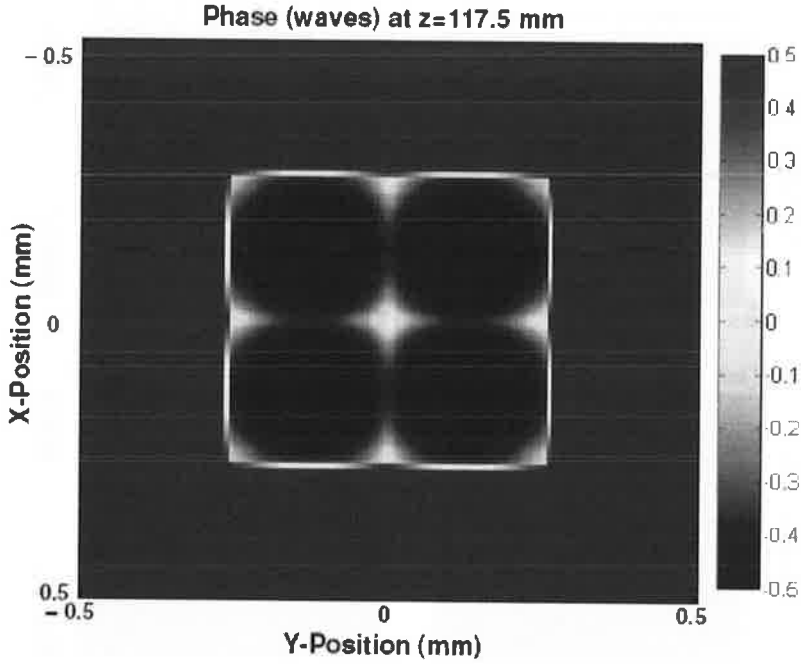

Fig. 2. Output phase map (in waves) of the beam splitter from Fig. 1. The four output beams have uniform phase.

cophased, the full re-imaging of the four beams requires at least one-fourth of the Talbot length.

3. Experimental Results

The 2-D architecture has been validated in proof-of-concept demonstrations using three different pairs of waveguides: a square-core optical fiber, a hollow metallic structure, and a square glass capillary. Figure 4 shows the diagram of the proof-of-concept variant that utilizes two hollow waveguides made of square glass capillaries. The first waveguide acts as a one-to-four beam splitter, wherein a single input beam produces a 2×2 array of axially symmetric "subimage" beams. These beams are subsequently close coupled into a second identical waveguide in order to recombine the beams and produce a single output beam. The images of the combined beam and intermediate four beams are also shown in Fig. 4. These experimental images are in excellent agreement with the theoretical model.

The results in Fig. 4 illustrate and verify that the same waveguide can be used as either a beam splitter or a coherent beam combiner, depending on experimental configuration. In fact, the quality of beam splitting can be used as a diagnostic tool to evaluate the performance of the waveguide. Figure 5 shows the cross section of the glass capillary used in the experimental demonstration presented in Fig. 4 along with an experimental three-dimensional (3-D) image of four beams produced as a result of one-to-four splitting of a diffraction-limited input beam. The high quality of the four output beams indicates that the capillary, used as a beam splitter, can be effectively used as a four-to-one beam combiner.

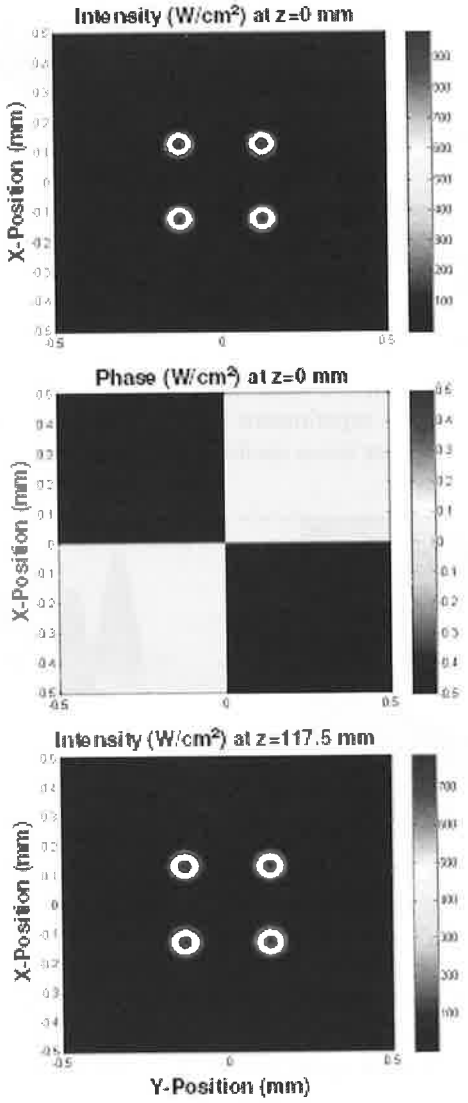

Fig. 3. Top: Four beams launched into the waveguide. Middle: Phase map of the four input beams, showing the diagonal beams with a half-wave phase shift. Bottom: Output profile of the waveguide.

To facilitate the launch of a 2×2 array of beams in such a configuration (on the order of 500 μm^2), and to accommodate the outputs of high-power fiber lasers in an all-fiber combiner module, several different types of fiber launch arrays were developed. Various fiber types and array configurations have been researched and tested for their power handling capabilities, single-mode quality, and ease of array fabrication. Figure 6 shows two examples of fiber arrays used in four-to-one beam combination. For initial demonstrations, standard Corning 980 PM single-mode fiber was used to create a serviceable array, with limitations to its power handling capability (Fig. 6, left-hand panel). A V-groove array was fabricated with

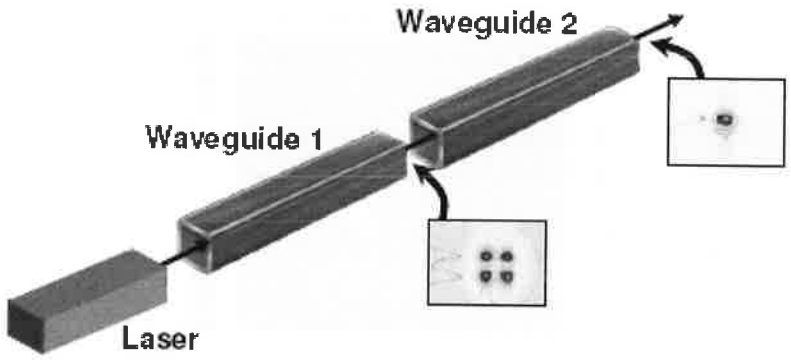

Fig. 4. Schematic diagram of the 2-D beam combiner module to combine four input beams into a single output beam. The experimental beam profiles demonstrate one-to-four beam splitting followed by four-to-one beam combining in a glass capillary waveguide.

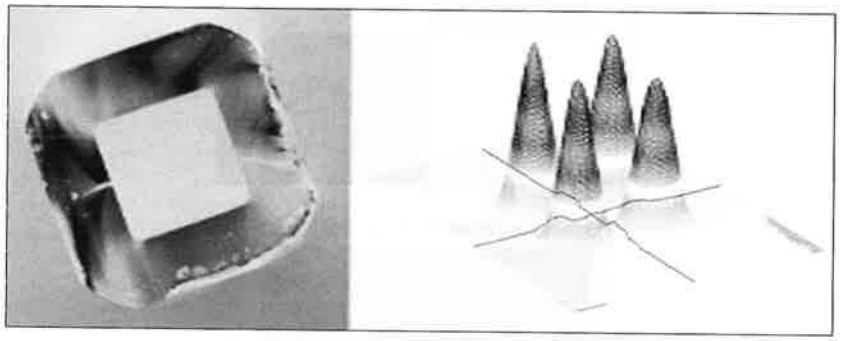

Fig. 5. Cross section of a 400-μm^2 glass capillary used as a beam-splitting or beam-combining waveguide (left) and an experimental output profile of four beams produced by splitting a single beam into four beams (right).

this single-mode fiber. Photonic crystal fiber (PCF) was chosen as a launch candidate for its single-mode propagation and, given its larger mode-field area, power-handling capabilities (Fig. 6, right-hand panel). Several square-groove arrays have been fabricated with different types of PCF.

The new 2-D REAPAR architecture was tested at low power (milliwatt) levels. A schematic diagram of the four-to-one coherent beam combiner is shown in Fig. 7. Because of the relatively large numerical aperture of the launch fibers, a microlens array made of antireflection coated fused silica was used to focus the four input beams into the glass capillary waveguide. The input beams at 1,064 nm were phase locked using a servo system equipped with fiber-coupled electro-optical and acousto-optical modulators used, respectively, for phase tagging and phase actuation.[4,8–10,14] The experimental 2-D and 3-D images of the combined output are shown in Fig. 8. These results were produced using the Corning 980 PM single-mode transport fiber V-groove array and a 0.5 × 0.5 mm glass capillary. The panels on the left-hand side of Fig. 8 show 2-D and 3-D images of the combiner output produced with the phases of the individual beams unlocked. The unlocked output shows that a considerable portion of the power is present in the eight sidelobes surrounding the central beam. The panels on the right-hand side show the output beam images produced

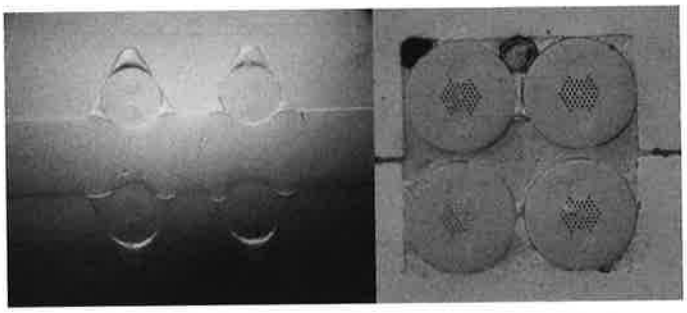

Fig. 6. 2 × 2 fiber arrays with fiber-to-fiber spacing of 250 μm. Left: V-groove PM 980 single-mode fiber array. Right: Square groove photonic crystal fiber array.

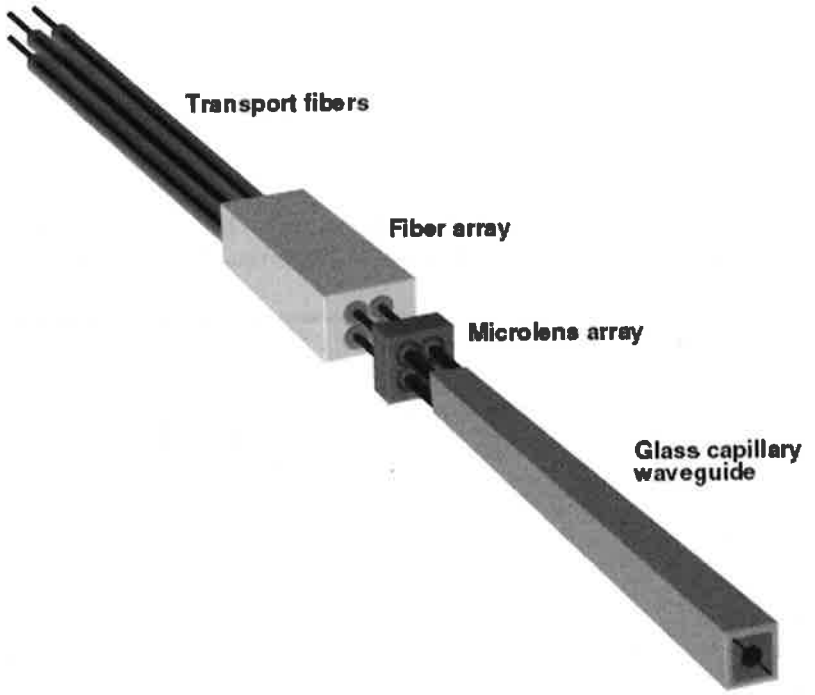

Fig. 7. Schematic diagram of the 2-D beam combiner module to combine four input beams into a single output beam.

with phase-locked input beams, where the eight sidelobes are nearly eliminated because of the cophasing.

The theoretically predicted four-beam output from the simulation with phase adjustment of the input beams was also tested. By adjusting the servo detection scheme, the servo can be forced to adjust the phases of the input beams. As opposed to a maximization of the central lobe in a typical beam-combining experiment, the servo was forced to maximize a corner lobe of the 3 × 3 output pattern. This resulted in the servo adjusting the phases of the input beams (giving two diagonal beams a half-wave offset) to produce the output shown in Fig. 9.

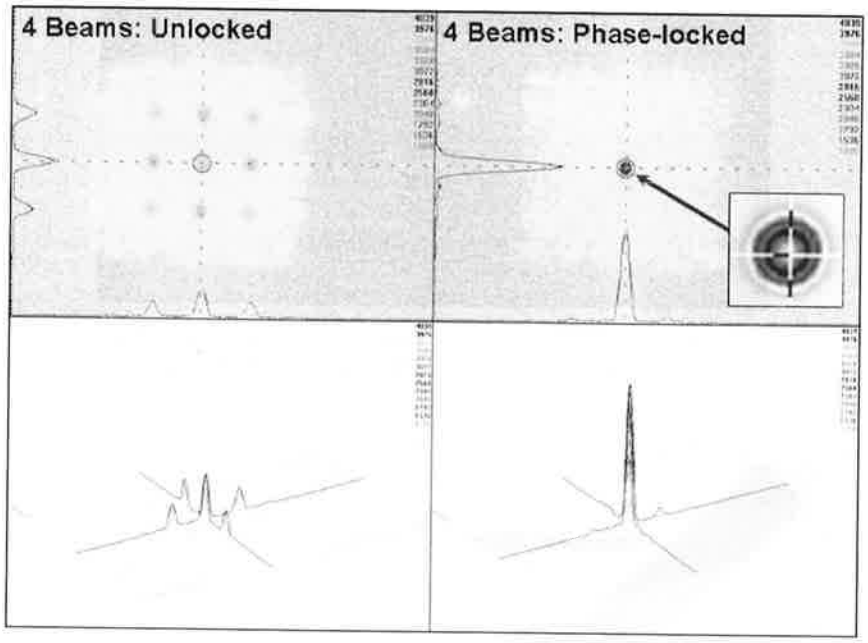

Fig. 8. 2-D and 3-D images of the glass capillary four-to-one combiner output with the phases of the four input beams unlocked (left-hand panels) and locked (right-hand panels).

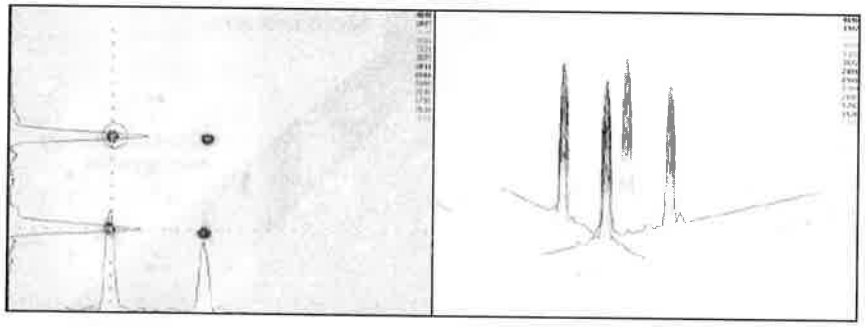

Fig. 9. The output of the beam combiner with the phases adjusted to re-image the input four beams.

4. Analysis

The insert in Fig. 8 shows the enlarged profile of the central lobe of the combined output. The central lobe power constitutes more than 90% of the total output power in the lobes; however, the total combining efficiency of the system is degraded by transmission losses and speckle background. The guiding mechanism within the capillary is Fresnel reflection from the air–glass interface at near glancing incidence. Because of the approximately 85%–90% reflection per "bounce" down the guide, approximately 65% of the input beams' power leaks into the walls of the capillary. Once in the walls of the capillary, the light makes another series of reflections back and forth between each glass–air interface, with some of the light exiting the system as losses (around 25% of the total input beam power)

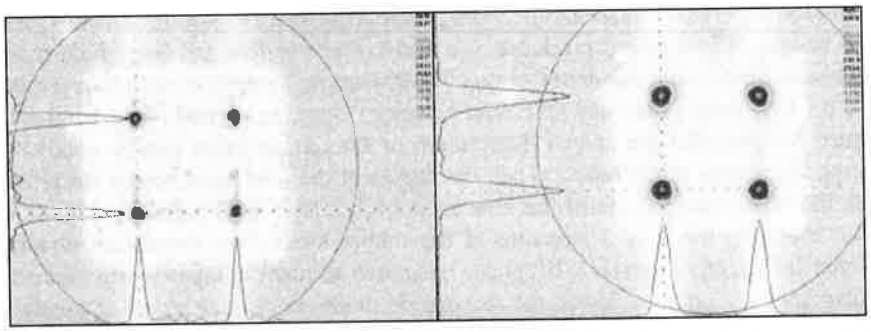

Fig. 10. Left: 2 × 2 splitting with single-mode fiber. Right: 2 × 2 splitting with PCF. Because of the smaller numerical aperture of the PCF, the input focusing conditions are optimized to improve transmission by ~15% and achieve nearly double the power in the lobes.

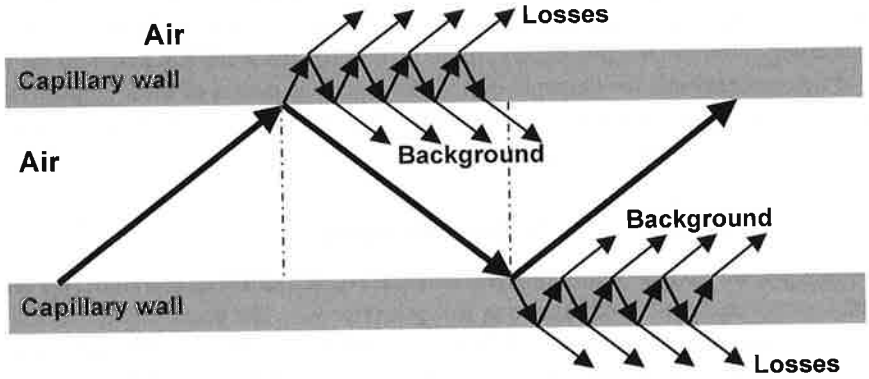

Fig. 11. Fresnel reflection at the air–glass interface of the capillary waveguide, resulting in transmission losses and speckle background.

and the rest refracting back into the waveguide. The light that reenters the waveguide no longer contributes to proper Talbot imaging and beam combination, merely showing up as a speckle background (see Figs. 8–10), which accounts for approximately 40% of the input power. The reflection scheme in the interior of the capillary walls is depicted in Fig. 11. This main inefficiency of the current capillary waveguide can be removed or significantly reduced by coating the waveguide interior with a highly reflective coating. This reflective coating will prevent leakage into the capillary wall, thus confining a majority of the light in the guide to contribute to beam combination. The combining efficiency can be also be improved by optimizing the focusing conditions of the input beams, i.e., by producing a larger focal spot and/or using transport fibers with a larger numerical aperture to further increase the incidence angle and thus enhance Fresnel reflections in the waveguide. An additional benefit of the increased input spot size is the increase in the length tolerance of the guide, as a larger spot size will have a significantly larger Rayleigh range (tolerances could go from hundreds of microns to millimeters as beam size increases from about 10 μm to about 40 μm). This improved efficiency was verified experimentally in a beam-splitting configuration, as using PCF with a lower numerical aperture produced better

transmission (by ~15%) and nearly doubled power in the lobes. Figure 10 shows experimental 2-D images of four beams produced as a result of one-to-four splitting of a diffraction-limited input beam using standard Corning 980 PM single-mode fiber with numerical aperture of 0.1 (left-hand panel) and PCF with numerical aperture of 0.04 (right-hand panel).

Figure 3 shows that the spatial distribution of the output beam can be controlled by adjusting the phases of the input. When the phases of the four input beams are arbitrarily varied, the relative brightness of the nine output lobes (left-hand panels in Fig. 3) varies without changing the 3 × 3 structure of the output lobes. Our simulation results also show that sufficiently large (~λ/10) phase mismatch among the input beams can produce irregular intensity patterns inside the waveguide, with occasional higher intensity spots located close to the walls of the waveguide. These "hot spots" could potentially lead to increased absorption and, perhaps, localized damage to the waveguide at sufficiently high powers. Although detailed discussion on scaling of the REAPAR technique to high powers is beyond the scope of this paper, it should be noted that with optimized focusing conditions of the input beams, more than 90% of the light launched into the waveguide reflects at the glancing incidence angles, regardless of the input phase configuration. The phase control servo system, which was used with the beam combiner, maintains the phase error to less than 0.06 deg. With an effective bandwidth of ~100 kHz, the servo can maintain the phase lock of the input beams, for example during the warm-up period of laser amplifiers, in a master oscillator power amplifier configuration, thus preventing formation of potentially dangerous, phase-dependent hot spots.

5. Conclusions

In summary, we have developed a novel scalable 2-D REAPAR architecture and demonstrated four-to-one beam combination at low power levels. The beam combiner design is based on inexpensive components, including a commercial off-the-shelf glass capillary waveguide and microlens array, as well as a new-design fiber array. Ongoing work on optimization of the beam combiner by coating the capillary and improving the fiber arrays is expected to both significantly improve the overall transmission of the system and reduce the speckle background. The optimized 2-D beam combiner will provide a scalable path to multikilowatt phased arrays with high fiber count, low loss, and negligible aberrations.

6. Acknowledgment

The authors would like to thank Dr. Sepp Unternahrer for helpful discussions and assistance in waveguide modeling. We gratefully acknowledge the support of the High Energy Laser–Joint Technology Office, which sponsored this research.

References

[1]Anderegg, J., J. Brosnan, E. Cheung, P. Epp, D. Hammons, H. Komine, M. Weber, and M. Wickham, Proc. SPIE **6102**, 1 (2006).

[2]Augst, S.J., A.K. Goyal, R.L. Aggarwal, T.Y. Fan, and A. Sanchez, Opt. Lett. **28**, 331 (2003).

[3]Augst, S.J., J.K. Ranka, and A. Sanchez, J. Opt. Soc. Am. B **24**(8), 1707 (2007).

[4]Bratcher, A., and R. Uberna, "Re-imaging Assisted Phased Array in a 2-Dimensional Hollow Waveguide," Solid State Diode Laser Technology Review, Albuquerque, NM, June 3–5, 2008.

[5]Bryngdahl, O., J. Opt. Soc. Am. **63**(4), 416 (1973).

[6]Bryngdahl, O., J. Opt. Soc. Am. **68**(3), 310 (1978).

[7]Cheung, E.C., J.G. Ho, G.D. Goodno, R.R. Rice, J. Rothenberg, P. Thielen, M. Weber, and M. Wickham, Opt. Lett. **33**, 354 (2008).

[8]Christensen, S., O. Koski, I. Lee, I.T. McKinnie, and J.R. Unternahrer, "Novel Coherent Beam Combiner," Solid State Diode Laser Technology Review, Albuquerque, NM, June 13–15, 2006.

[9]Christensen, S., O. Koski, I. Lee, I.T. McKinnie, and J.R. Unternahrer, "2-Dimensional Re-imaging Assisted Phased Array Progress," Solid State Diode Laser Technology Review, Los Angeles, CA, June 26–28, 2007.

[10]Christensen, S., I.T. McKinnie, and S.J. Unternahrer, "Method and Apparatus to Coherently Combine High-Power Beams in Self-Imaging Waveguides," U.S. Patent 7239777, 2007.

[11]Ciapurin, I.V., V.I. Smirnov, and L.B. Glebov, "High-Density Spectral Beam Combining by Thick PTR Bragg Gratings," Solid State Diode Laser Technology Review, 2004, Paper BEAM-4.

[12]Corcoran, C.J., Appl. Phys. Lett. **86**, 201118 (2005).

[13]Fan, T.Y., IEEE J. Selected Topics Quantum Electron. **11**(3), 567 (2005).

[14]Goodno, G.D., C.P. Asman, J. Anderegg, S. Brosnan, E.C. Cheung, D. Hammons, H. Injeyan, H. Komine, W.H. Long, M. McClellan, S.J. McNaught, S. Redmond, R. Simpson, J. Sollee, M. Weber, S.B. Weiss, and M. Wickham, IEEE J. Selected Topics Quantum Electron. **13**(3), 460 (2007).

[15]Goodno, G.D., H. Komine, S.J. McNaught, S.B. Weiss, S. Redmond, W. Long, R. Simpson, E.C. Cheung, D. Howland, P. Epp, M. Weber, M. McClellan, J. Sollee, and H. Injeyan, Opt. Lett. **31**, 1247 (2006).

[16]Goodno, G.D., and J. Rothenberg, "Advances and Limitations in Fiber Laser Beam Combination," Frontiers in Optics 2008/Laser Science (LS) XXIV, Rochester, NY, October 19–23, 2008.

[17]Kozlov, V.A., J. Hernandez-Cordero, and T.F. Morse, Opt. Lett. **24**, 1814 (1999).

[18]Loftus, T.H., A.M. Thomas, P.R. Hoffman, M. Norsen, R. Royse, A. Liu, and E. Honea, IEEE J. Selected Topics Quantum Electron. **13**(3), 487 (2007).

[19]Morris, J., "Aerospace Daily: Keeping Cool a Big Challenge for JSF Laser, Lockheed Martin Says," Aerospace Daily, September 26, 2002. http://web.archive.org/web/20040604124353/http://www.aviationnow.com/avnow/news/channel_military.jsp?view=story&id=news/masd0926.xml,

[20]Shay, T.M., V. Benham, J.T. Baker, B. Ward, A.D. Sanchez, M.A. Culpepper, D. Pilkington, J. Spring, D.J. Nelson, and C.A. Lu, Opt. Express **14**, 12015 (2006).

[21]Talbot, H.F., London Edinburgh Philosoph. Mag., J. Sci. **9**, 401 (1836).

[22]Ulrich, R., and G. Ankele, Appl. Phys. Lett. **27**(6), 337 (1975).

The Authors

Mr. Andrew Bratcher obtained a B.S. (2004) and an M.S. (2007) in physics from the University of Arkansas in Fayetteville. He has worked with Dr. Gregory Salamo on the nonlinear interaction of light with photorefractive crystals. Currently, he is a research engineer at Lockheed Martin Coherent Technologies in Louisville, Colorado, where he works with Dr. R. Uberna on coherent beam combination methods and polarization management in optical systems.

Dr. Radoslaw (Radek) Uberna obtained a M.S. in chemistry from Jagiellonian University in Krakow, Poland, in 1990 and a Ph.D. in chemical physics from the University of Nevada, Reno, in 1996. He has worked with Dr. Joe I. Cline on measurement and control of the correlations between velocity, angular momentum, and transition dipole moment vectors in photofragmentation products. As a Postdoctoral Fellow at JILA, University of Colorado at Boulder (1997–2000), he worked with Dr. Stephen R. Leone on quantum control of photophysical processes in molecules using phase- and amplitude-shaped femtosecond pulses. As a Senior Optical Scientist at Meadowlark Optics, he designed and built new ellipsometers and liquid crystal optical devices. In 2003, he cofounded Optical Finesse, where he developed novel Stokes and Mueller polarimeters and other optical instruments for biomedical research. Currently, as a Research Scientist at Lockheed Martin Coherent Technologies, Louisville, Colorado, he works on coherent beam combination and polarization management in optical systems.